Ex. 1

Kpl.

DET NORSKE VIDENSKAPS-AKADEMI I OSLO

GEOFYSISKE PUBLIKASJONER
GEOPHYSICA NORVEGICA

V. 26
1965-67

Vol. XXVI. No. 1 February 1965

EIGIL HESSTVEDT

Some characteristics of the oxygen-hydrogen atmosphere

DET NORSKE METEOROLOGISKE INSTITUTT
BIBLIOTEKET
BLINDERN, OSLO 3

OSLO 1965
UNIVERSITETSFORLAGET

GEOFYSISKE PUBLIKASJONER

GEOPHYSICA NORVEGICA

VOL. XXVI. NO. 1

SOME CHARACTERISTICS OF THE OXYGEN-HYDROGEN ATMOSPHERE

By Eigil Hesstvedt

FREMLAGT I VIDENSKAPS-AKADEMIETS MØTE DEN 22. MAI 1964 AV ELIASSEN

TRYKT MED BIDRAG FRA NORGES ALMENVITENSKAPELIGE FORSKNINGSRÅD

Summary. On the basis of a system of chemical reactions the concentrations of O, O_2, O_3, OH, HO_2, H_2, H_2O and H are computed for elevations between 35 km and 140 km. Equilibrium concentrations for daytime conditions as well as characteristic times for restoration of photochemical equilibrium are found for three temperature profiles: low latitude and high latitude summer and winter. Similar computations are made by considering the diurnal variation in solar radiation. Atmospheric hydrogen is found to be mainly in the form of atomic hydrogen above 95 km, in the form of molecular hydrogen between 70 km and 95 km, and in the form of water vapor below 70 km. As a result of the computations the intensity of the OH* emission in the airglow is determined. Maximum dayglow emission is found at about 55 km. The maximum OH* nightglow emission lies between 80 km and 100 km, depending on latitude and season. All the computations are made for a static atmosphere model. It is suggested that the atmospheric circulation is likely to modify considerably the results obtained for the static model.

1. Introduction. Construction of photochemical model atmospheres has turned out to be a very useful tool in the study of many problems concerning the physics of the high atmosphere. The simplest of such model atmospheres, the pure oxygen atmosphere, has been studied by various authors (see for instance Hesstvedt, 1963). Spatial distribution of the concentrations of the three oxygen allotropes O, O_2 and O_3 has been evaluated theoretically and the results are in reasonable agreement with observational data for most atmospheric levels.

An important step forward in the development of photochemical model atmospheres was made when Bates and Nicolet (1950) introduced hydrogen into the model. Their fundamental work has made it possible to evaluate theoretically the distribution with height, latitude and season of the most important hydrogen and oxygen compounds. Furthermore, the effect of the presence of hydrogen upon the pure oxygen components may be evaluated.

Later some particular aspects of the oxygen-hydrogen atmosphere have been investigated in more detail. The OH*-emission in the nightglow has been studied by Wallace (1962) and Ballif and Venkateswaran (1963), and the water vapor

content in the high atmosphere has been investigated by HESSTVEDT (1964). All these works have used the chemical reactions proposed by BATES and NICOLET. During the last decade our knowledge about the temperature and pressure in the high atmosphere and their variations with height, latitude and season has improved considerably. Furthermore, many of the values of the recombination rates for the chemical reactions involved in the model, as well as the dissociation rates, determined from ultra-violet solar radiation data, have recently been revised.

In this paper the composition of the oxygen-hydrogen model atmosphere as a function of height, latitude, season and time of the day will be studied using new observational data. On the basis of the obtained concentrations for the various compounds the OH*-emission in the airglow will be discussed.

2. Photochemical reactions in the oxygen-hydrogen atmosphere model. In agreement with BATES and NICOLET we shall assume a model atmosphere where the following eight compounds are allowed to interact chemically: O, O_2, O_3, OH, HO_2, H_2, H_2O and H. In addition, our model atmosphere shall contain nonreacting elements, denoted below by M, which will act as third bodies in three-body collisions.

The following 24 reactions are considered between these compounds:

(2.1)	$O+O+M\rightarrow O_2+M$	$k_1 = 1.6\times10^{-34}\cdot T^{1/2}\text{cm}^6\text{sec}^{-1}$
(2.2)	$O+O_2+M\rightarrow O_3+M$	$k_2 = 6.4\times10^{-36}\cdot T^{1/2}\text{cm}^6\text{sec}^{-1}$
(2.3)	$O+O_3\rightarrow 2O_2$	$k_3 = 4.2\times10^{-13}\cdot T^{1/2}e^{-3.2/RT}\text{cm}^3\text{sec}^{-1}$
(2.4)	$O_2+h\nu\rightarrow 2O$	$J_2 = 5\times10^{-7}\text{sec}^{-1}$ for zero optical depth
(2.5)	$O_3+h\nu\rightarrow O+O_2$	$J_3 = 10^{-2}\text{sec}^{-1}$ for zero optical depth
(2.6)	$H+O+M\rightarrow OH+M$	$k_6 = 6\times10^{-34}\cdot T^{1/2}\text{cm}^6\text{sec}^{-1}$
(2.7)	$H+O_2+M\rightarrow HO_2+M$	$k_7 = 1.3\times10^{-33}\cdot T^{1/2}\text{cm}^6\text{sec}^{-1}$
(2.8)	$H+O_3\rightarrow OH+O_2$	$k_8 = 8\times10^{-12}\cdot T^{1/2}e^{-1/RT}\text{cm}^3\text{sec}^{-1}$
(2.9)	$H+O_3\rightarrow HO_2+O$	$k_9 = 1.5\times10^{-11}\cdot T^{1/2}e^{-4/RT}\text{cm}^3\text{sec}^{-1}$
(2.10)	$OH+O\rightarrow H+O_2$	$k_{10} = 6.7\times10^{-12}\cdot T^{1/2}e^{-0.5/RT}\text{cm}^3\text{sec}^{-1}$
(2.11)	$HO_2+O\rightarrow OH+O_2$	$k_{11} = 6\times10^{-13}\cdot T^{1/2}\text{cm}^3\text{sec}^{-1}$
(2.12)	$HO_2+h\nu\rightarrow OH+O$	$J_{12} = 10^{-4}\text{sec}^{-1}$
(2.13)	$H_2O+h\nu\rightarrow OH+H$	$J_{13} = 1.5\times10^{-5}\text{sec}^{-1}$ for zero optical depth
(2.14)	$H+HO_2\rightarrow H_2O+O$	$k_{14} = 1.5\times10^{-11}\cdot T^{1/2}e^{-4/RT}\text{cm}^3\text{sec}^{-1}$
(2.15)	$H+HO_2\rightarrow H_2+O_2$	$k_{15} = 1.9\times10^{-13}\cdot T^{1/2}\text{cm}^3\text{sec}^{-1}$
(2.16)	$H+HO_2\rightarrow 2OH$	$k_{16} = 6\times10^{-13}\cdot T^{1/2}\text{cm}^3\text{sec}^{-1}$

(2.17) $H+H+M \rightarrow H_2+M$ $\quad k_{17}=1.6\times10^{-33}\cdot T^{1/2}\text{cm}^6\text{sec}^{-1}$

(2.18) $H+OH \rightarrow H_2+O$ $\quad k_{18}=1.5\times10^{-11}\cdot T^{1/2}e^{-4/RT}\text{cm}^3\text{sec}^{-1}$

(2.19) $H_2+O \rightarrow OH+H$ $\quad k_{19}=4.5\times10^{-11}\cdot T^{1/2}e^{-7/RT}\text{cm}^3\text{sec}^{-1}$

(2.20) $H_2+OH \rightarrow H_2O+H$ $\quad k_{20}=7\times10^{-12}\cdot T^{1/2}e^{-10/RT}\text{cm}^3\text{sec}^{-1}$

(2.21) $OH+O_3 \rightarrow HO_2+O_2$ $\quad k_{21}=1.5\times10^{-11}\cdot T^{1/2}e^{-4/RT}\text{cm}^3\text{sec}^{-1}$

(2.22) $H+O_2 \rightarrow OH+O$ $\quad k_{22}=3.6\times10^{-9}\cdot T^{1/2}e^{-24/RT}\text{cm}^3\text{sec}^{-1}$

(2.23) $OH+OH \rightarrow H_2O+O$ $\quad k_{23}=1.6\times10^{-13}\cdot T^{1/2}\text{cm}^3\text{sec}^{-1}$

(2.24) $OH+HO_2 \rightarrow H_2O+O_2$ $\quad k_{24}=6\times10^{-13}\cdot T^{1/2}\text{cm}^3\text{sec}^{-1}$

Here $k_1, k_2, \ldots k_{24}$ are the rate coefficients for the recombination processes, and $\mathcal{J}_2$, $\mathcal{J}_3$, $\mathcal{J}_{12}$ and $\mathcal{J}_{13}$ are dissociation rates.

The time variations of the concentrations of the eight components are then given by eight differential equations.

(2.25) $$\frac{d[O]}{dt}=A_1-B_1[O]-C_1[O]^2$$

(2.26) $$\frac{d[O_2]}{dt}=A_2-B_2[O_2]$$

(2.27) $$\frac{d[O_3]}{dt}=A_3-B_3[O_3]$$

(2.28) $$\frac{d[OH]}{dt}=A_4-B_4[OH]-C_4[OH]^2$$

(2.29) $$\frac{d[HO_2]}{dt}=A_5-B_5[HO_2]$$

(2.30) $$\frac{d[H_2]}{dt}=A_6-B_6[H_2]$$

(2.31) $$\frac{d[H_2O]}{dt}=A_7-B_7[H_2O]$$

(2.32) $$\frac{d[H]}{dt}=A_8-B_8[H]-C_8[H]^2$$

Brackets [ ] are used to denote the particle concentrations of the components. The coefficients A_i, B_i and C_i are functions of these concentrations, but in each equation the coefficients are independent of the concentration of the dependent variable.

The equations (2.25) through (2.32) also include the relations

$$[O_2]+[HO_2]+\tfrac{1}{2}([O]+3[O_3]+[H_2O])=\alpha[M] \tag{2.33}$$

$$[H_2]+[H_2O]+\tfrac{1}{2}([OH]+[HO_2]+[H])=\beta[M] \tag{2.34}$$

expressing that the relative concentrations oxygen (total amount) to air and hydrogen (total amount) to air are constant at a given height. As is usually done we shall assume $\alpha=0.2095$ for all levels. The selection of representative values of β is considerably more difficult. As will be shown later, practically all hydrogen below 70 km is in the form of water vapor. Accordingly our choice of a value for β should depend upon stratospheric humidity measurements. In this paper we shall assume $\beta=2.4\times10^{-4}$ corresponding to a mixing ratio of $1.5\times10^{-4}g/g$, proposed by GUTNICK (1962) for the 30 km level.

Since all the rate coefficients $k_1, k_2, \ldots k_{24}$ depend upon the temperature, and since [M] is a function of temperature and pressure, we have to specify a temperature and pressure profile for our model atmosphere. Due to seasonal and latitudinal temperature variations, which are especially pronounced near the mesopause, it is necessary to select at least three different profiles. NORDBERG and STROUD (1961) have computed mean temperatures for low latitudes (year) and for high latitudes (winter and summer separately). Their profiles were, with a slight revision, selected for the present calculations. (See table 1.)

Table 1. *Assumed temperature profiles for low and high latitudes, summer and winter.*

Height, km	Low latitude, summer and winter	High latitude, summer	High latitude, winter
140	712°K	712°K	712°K
130	531	531	531
120	350	350	350
110	257	257	270
105	236	232	256
100	218	212	242
95	203	196	231
90	190	178	223
85	185	161	217
80	190	163	215
75	200	188	219
70	219	212	225
60	247	254	252
50	270	274	259
40	254	254	230
35	240	244	217

The dissociation rates J_2 and J_3 have been determined by DÜTSCH (1956) and NICOLET (1958) as functions of the total amount of O_2 and O_3 in the overlying part of the atmosphere in the path of the sun's rays. Their values were used in the calculations in this paper. Dissociation of HO_2 is caused by radiation in the visible part of the spectrum. Consequently the absorption of the dissociating radiation is negligibly small and J_{12} may be taken as a constant. The dissociation rate for H_2O was calculated on the basis of recent radiation data (FRIEDMAN, 1961, NAWROCKI and PAPA, 1961, WATANABE, 1958). Dissociation of H_2O takes place in two parts of the spectrum, in the 1500-1900 Å continuum and by Lyα radiation. The Lyα radiation was found to contribute significantly to the dissociation rate down to 60 km in low latitudes, down to 65 km in the high latitudes summer and down to 75 km in the high latitudes winter. It was found that for zero optical depth one third ($5 \times 10^{-1}\text{sec}^{-6}$) of the total dissociation rate was due to Lyα radiation.

The optical depth depends strongly upon the elevation of the sun. Therefore we have to specify representative mean values for our three model atmospheres. In low latitudes the sun was assumed to be in zenith during daytime. For high (60°) latitude, midsummer, the mean elevation during daytime was assumed to be 30°, and for high latitude, winter, the mean elevation during the day was taken as 4.5°.

3. The pure oxygen atmosphere. The characteristics of the pure oxygen model atmosphere have been studied by various authors (see for instance HESSTVEDT, 1963). In these investigations the values of the recombination coefficient k_3 differed considerably

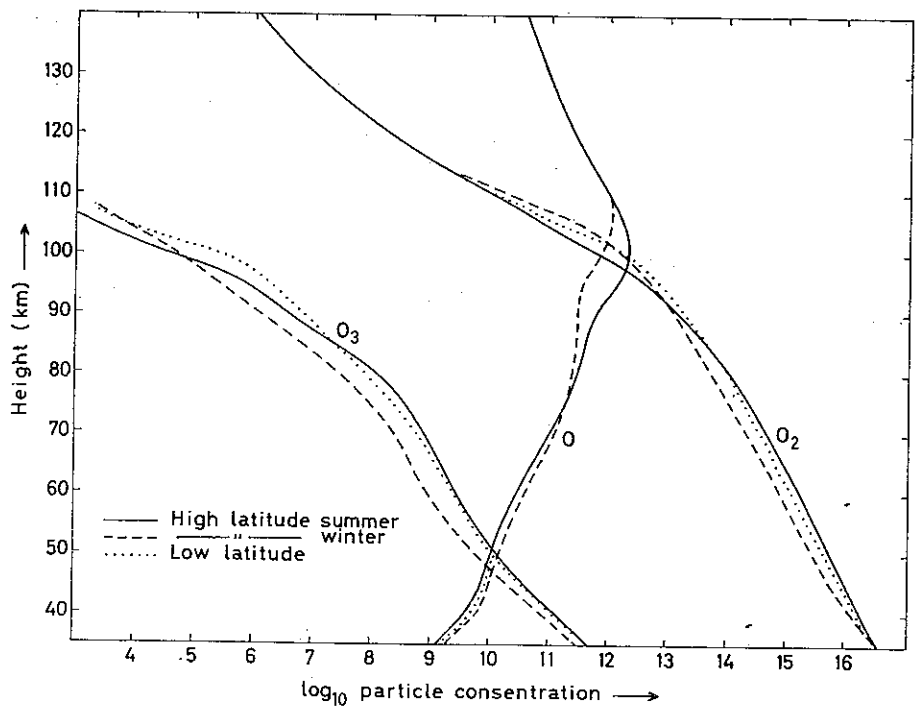

Figure 1. Daytime equilibrium concentrations in a pure oxygen atmosphere.

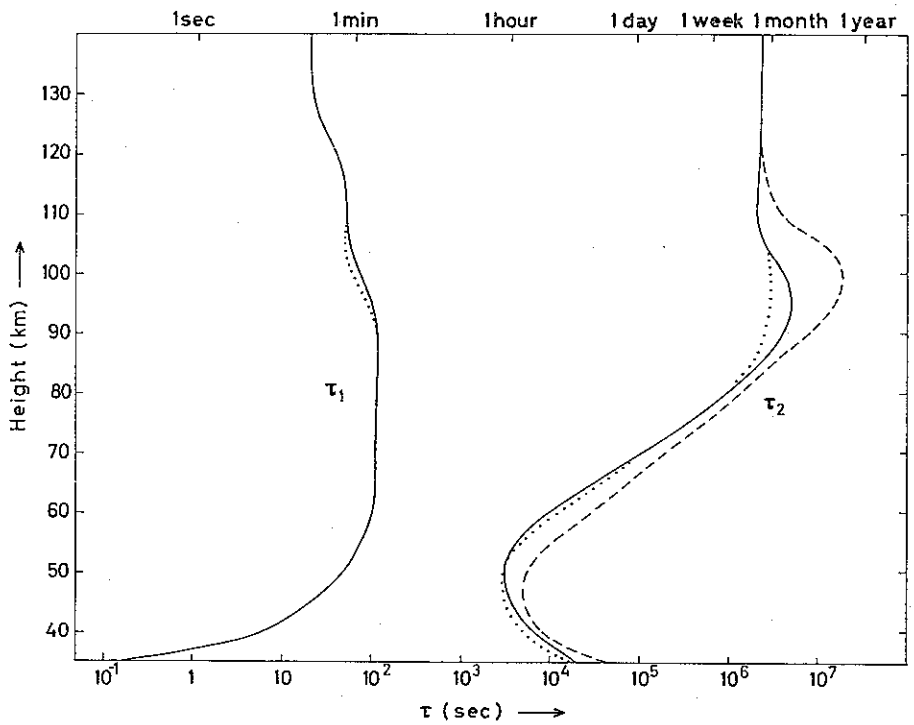

Figure 2. Characteristic times in a pure oxygen atmosphere (solid curve: high latitude summer, broken curve: high latitude winter, dotted curve: low latitude).

from that given in section 2 of this paper. Since it is of interest to compare the equilibrium values and the characteristic times in the pure oxygen atmosphere to those in the oxygen-hydrogen atmosphere, new computations have been made using the revised value of k_3. The results of such computations are shown in figures 1 and 2. A comparison with earlier results (HESSTVEDT, 1963) shows that the revision required by the new selection of k_3-value is relatively small.

4. Daytime equilibrium concentrations in the oxygen-hydrogen atmosphere. Equilibrium concentrations for mean daytime conditions may be computed for the three model atmospheres defined by table 1 by assuming that the time variations in equations (2.25) through (2.32) are zero. The resulting system of eight equations in combination with (2.33) and (2.34) was solved by an iterative method for each level and for the three atmospheric models defined in table 1. The results of such computations are shown in figure 3-5.

Figure 3 shows the daytime equilibrium concentrations of the pure oxygen components. In order to evaluate the effect of introducing hydrogen into the model atmosphere, figure 3 should be compared to figure 1. It is seen that this effect is negligibly small above about 95 km and below about 55 km. The concentration of O_2 is never affected by the introduction of hydrogen, whereas the concentration of O (and consequently the concentration of O_3, since these are nearly proportional) is considerably

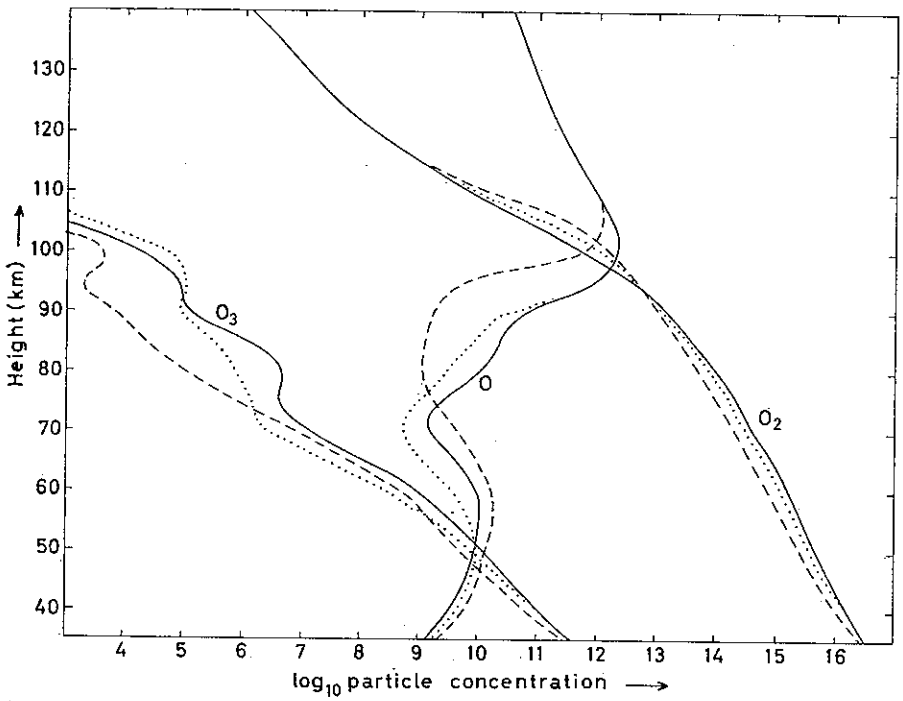

Figure 3. Daytime equilibrium concentrations of O, O_2 and O_3 in an oxygen-hydrogen atmosphere (solid curve: high latitude summer, broken curve: high latitude winter, dotted curve: low latitude).

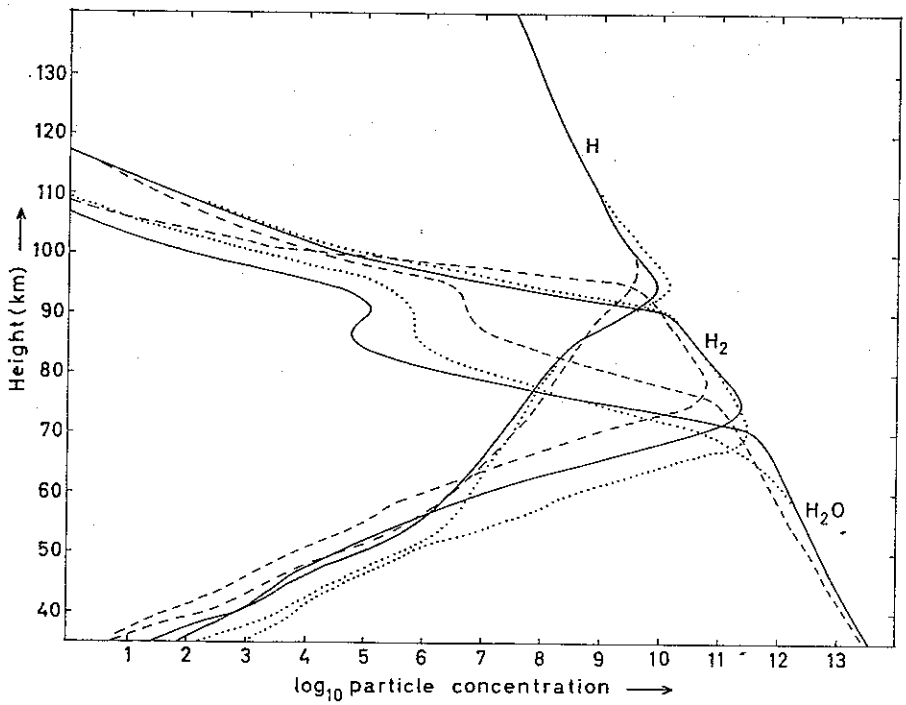

Figure 4. Daytime equilibrium concentrations of H, H_2 and H_2O in an oxygen-hydrogen atmosphere (solid curve: high latitude summer, broken curve: high latitude winter, dotted curve: low latitude).

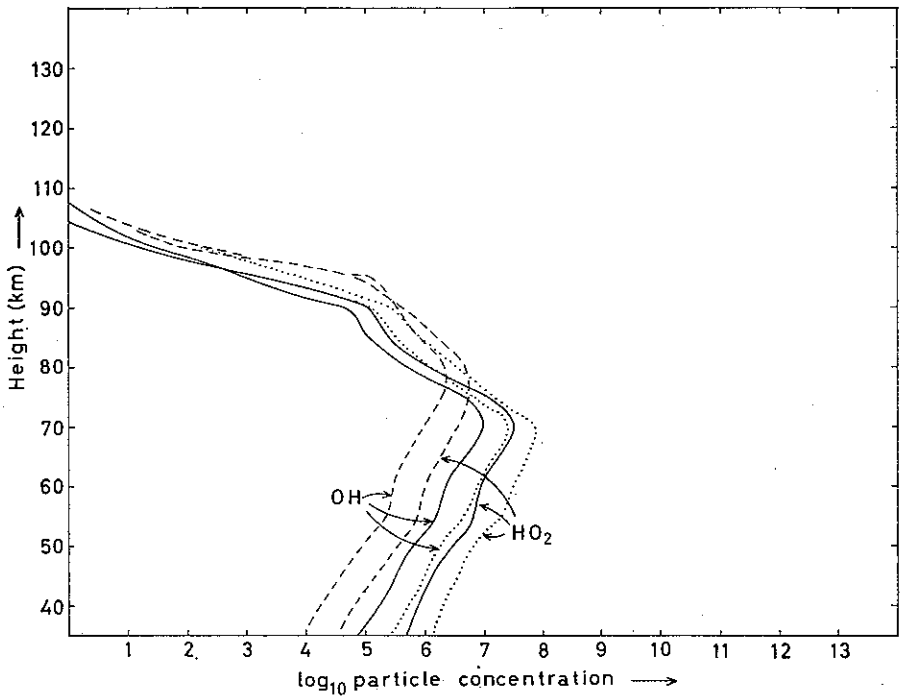

Figure 5. Daytime equilibrium concentrations of OH and HO_2 in an oxygen-hydrogen atmosphere (solid curve: high latitude summer, broken curve: high latitude winter, dotted curve: low latitude).

reduced between 55 and 95 km. The magnitude of this reduction depends upon the value selected for β. For the value of β used in the present work, the reduction amounts to one to two orders of magnitude. The reduction of atomic oxygen is not accounted for by a specific recombination process, but rather by a complex chain of reactions ending up in the formation of water vapor or in a recombination to molecular oxygen. (The increase in the concentration of O_2 is, of course, unimportant since the concentrations of O and O_2 differ by orders of magnitude).

Daytime equilibrium concentrations for the pure hydrogen and oxygen-hydrogen compounds are shown in figures 4 and 5. It is seen that practically all atmospheric hydrogen is in the form of H above about 95 km. Roughly between the levels 75 and 95 km, H_2 takes up the major part of the hydrogen. Below about 70 km the distribution of hydrogen is completely dominated by water vapor. OH and HO_2 are seen to be minor constituents at all levels.

It is of interest to compare the vertical distributions of the concentrations of the hydrogen compounds, as illustrated in figures 4 and 5, to the results obtained earlier for the levels 65 to 95 km by BATES and NICOLET (1950). According to these authors, atomic hydrogen is the dominating component above about 75 km, while water vapor takes up most of the hydrogen below about 68 km. Between these levels molecular hydrogen enters the picture, and roughly we may say that the hydrogen is evenly distributed on H, H_2 and H_2O. Also BATES and NICOLET concluded that OH and HO_2 are minor constituents at all levels.

5. Characteristic times in a sunlit oxygen-hydrogen atmosphere. The concentrations of the eight components of our oxygen-hydrogen atmosphere model, derived in section 3, refer to equilibrium conditions corresponding to a constant solar radiation and to an atmosphere without motion or diffusion. Such conditions are never fullfilled in the real atmosphere. The radiation from the sun varies with the time of the day, while the circulation of the atmosphere brings air from one level or latitude to another where the equilibrium conditions may be different. Consequently departures from photochemical equilibrium may be expected. If the equilibrium is a stable one the departures approach zero with time. The time required to reduce the departure to $1/e$ times its initial value is called the characteristic time for the component in question.

If A and B are constants, the differential equation

$$\frac{dx}{dt}=A-Bx \tag{5.1}$$

has the solution

$$x=x_e+(x_0-x_e)e^{-Bt} \tag{5.2}$$

where x_0 is the value of x for $t=0$ and $x_e=A/B$ is the value for $t\to\infty$. The time required for the difference $x-x_e$ to reduce to $1/e$ times its initial value (i.e. the characteristic time for the quantity x) is then $1/B$. An analogous result is obtained if the expression on the right hand side of (5.1) is of second degree in x.

If the coefficients in expressions (2.25) to (2.32) are regarded as constants, the equations may be integrated and the characteristic times determined. For instance, the characteristic time for H_2O would be determined as $1/B_7=1/\mathcal{J}_{13}$. This procedure, which is commonly used, will in general lead to representative values. However, the assumption of constant coefficients is in many cases a very crude one, and the value obtained for the characteristic times in this way may be completely misleading. In order to avoid these difficulties we shall transform equations (2.25) through (2.32) by substituting

$$\begin{aligned}
[O] &= [O]_e+[O]' \\
[O_2] &= [O_2]_e+[O_2]' \\
[O_3] &= [O_3]_e+[O_3]' \\
[OH] &= [OH]_e+[OH]' \\
[HO_2] &= [HO_2]_e+[HO_2]' \\
[H_2] &= [H_2]_e+[H_2]' \\
[H_2O] &= [H_2O]_e+[H_2O]' \\
[H] &= [H]_e+[H]'
\end{aligned} \tag{5.3}$$

where index e is used to denote equilibrium values and dashes denote departures from photochemical equilibrium. It follows that equations (2.33) and (2.34) may be transformed to

$$[O_2]' = -[HO_2]' - \tfrac{1}{2}([O]' + 3[O_3]' + [OH]' + [H_2O]') \tag{5.4}$$

and

$$[H]' = -2([H_2]' + [H_2O]') - [OH]' - [HO_2]' \tag{5.5}$$

Substitution of (5.3), (5.4) and (5.5) in equations (2.25), (2.27), (2.28), (2.29), (2.30) and (2.31) yields six differential equations in the perturbations of the concentrations of O, O_3, OH, HO_2, H_2 and H_2O. In the following computations we shall assume that these perturbations are small in comparison to the equilibrium values, so that product terms of the perturbations may be neglected as second order terms. In this way we obtain six linear differential equations of the type

$$\frac{dx_i}{dt} = a_{i1}x_1' + a_{i2}x_2' + a_{i3}x_3' + a_{i4}x_4' + a_{i5}x_5' + a_{i6}x_6' \tag{5.6}$$

(i = 1, 2 . . . 6). The solutions to this set of equations are of the form

$$x_i = \sum_{j=1}^{6} b_{ji} e^{-\lambda_j t} \tag{5.7}$$

where $\lambda_1, \lambda_2, \ldots \lambda_6$ are the roots of the equation

$$\begin{vmatrix} a_{11}+\lambda & a_{12} & a_{13} & a_{14} & a_{15} & a_{16} \\ a_{21} & a_{22}+\lambda & a_{23} & a_{24} & a_{25} & a_{26} \\ a_{31} & a_{32} & a_{33}+\lambda & a_{34} & a_{35} & a_{36} \\ a_{41} & a_{42} & a_{43} & a_{44}+\lambda & a_{45} & a_{46} \\ a_{51} & a_{52} & a_{53} & a_{54} & a_{55}+\lambda & a_{56} \\ a_{61} & a_{62} & a_{63} & a_{64} & a_{65} & a_{66}+\lambda \end{vmatrix} = 0 \tag{5.8}$$

The general solutions of our equations may consequently be written as

$$[0]' = \sum_{j=1}^{6} b_{j1} e^{-\lambda_j t} \tag{5.9}$$

$$[O_2]' = \sum_{j=1}^{6} b_{j2} e^{-\lambda_j t} \tag{5.10}$$

$$[O_3]' = \sum_{j=1}^{6} b_{j3} e^{-\lambda_j t} \tag{5.11}$$

$$[OH]' = \sum_{j=1}^{6} b_{j4} e^{-\lambda_j t} \tag{5.12}$$

$$[HO_2]' = \sum_{j=1}^{6} b_{j5} e^{-\lambda_j t} \tag{5.13}$$

$$[H_2]' = \sum_{j=1}^{6} b_{j6} e^{-\lambda_j t} \tag{5.14}$$

$$[H_2O]' = \sum_{j=1}^{6} b_{j7} e^{-\lambda_j t} \tag{5.15}$$

$$[H]' = \sum_{j=1}^{6} b_{j8} e^{-\lambda_j t} \tag{5.16}$$

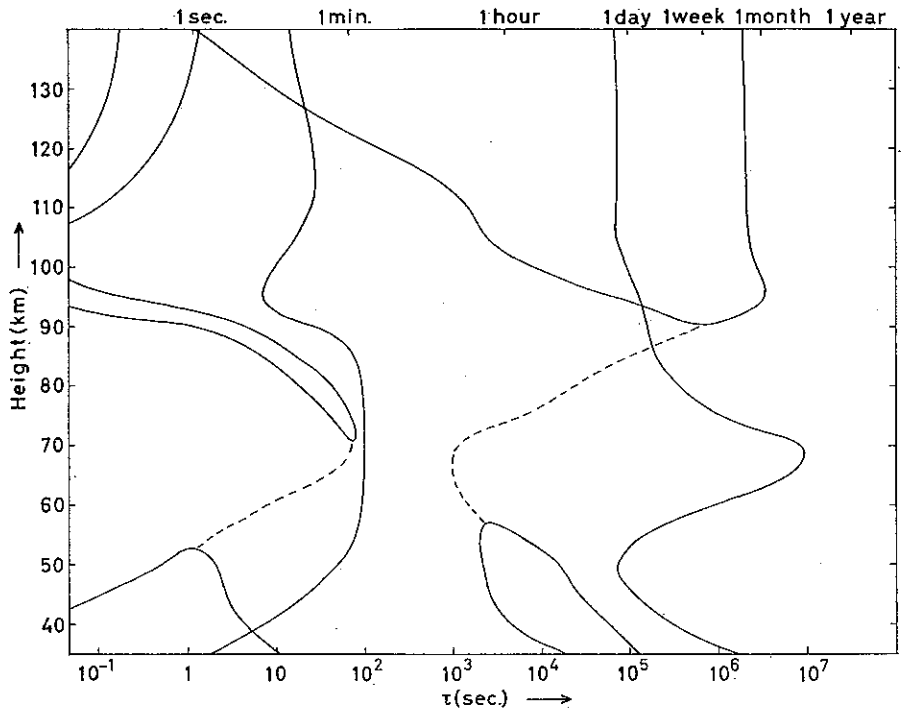

Figure 6. Characteristic times for an oxygen-hydrogen atmosphere (low latitude, daytime conditions).

The coefficients b_{ji} are constants which depend upon the value of the initial perturbations. The characteristic times of the system are now defined as $\tau_j = 1/\lambda_j$ $(j = 1, 2, \ldots 6)$.

Equation (5.8) was solved on an IBM 1620 computer for every fifth kilometer level between 35 and 140 km and for the three model atmospheres defined in table 1. The results are shown in figures 6-8.

Above 95 km and below 50 km six real, positive roots were obtained, showing that the equilibrium is a stable one. At levels between 50 and 95 km only two or four real roots were obtained, the remaining roots being complex. In the case of complex roots the real part was always found to be positive showing that the restoration of

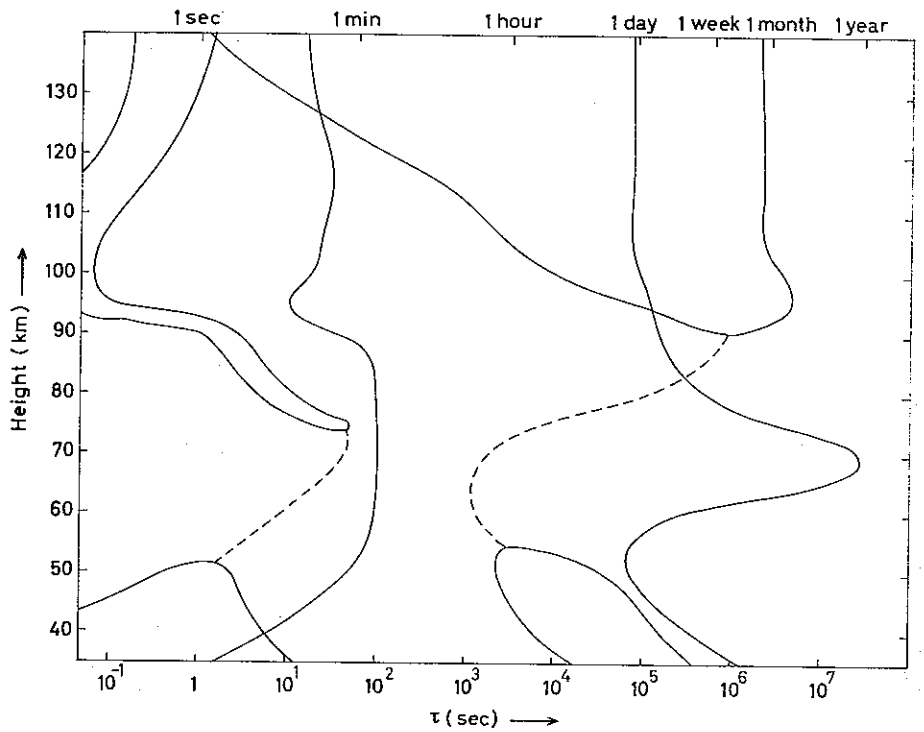

Figure 7. Characteristic times for an oxygen-hydrogen atmosphere (high latitude summer, daytime conditions).

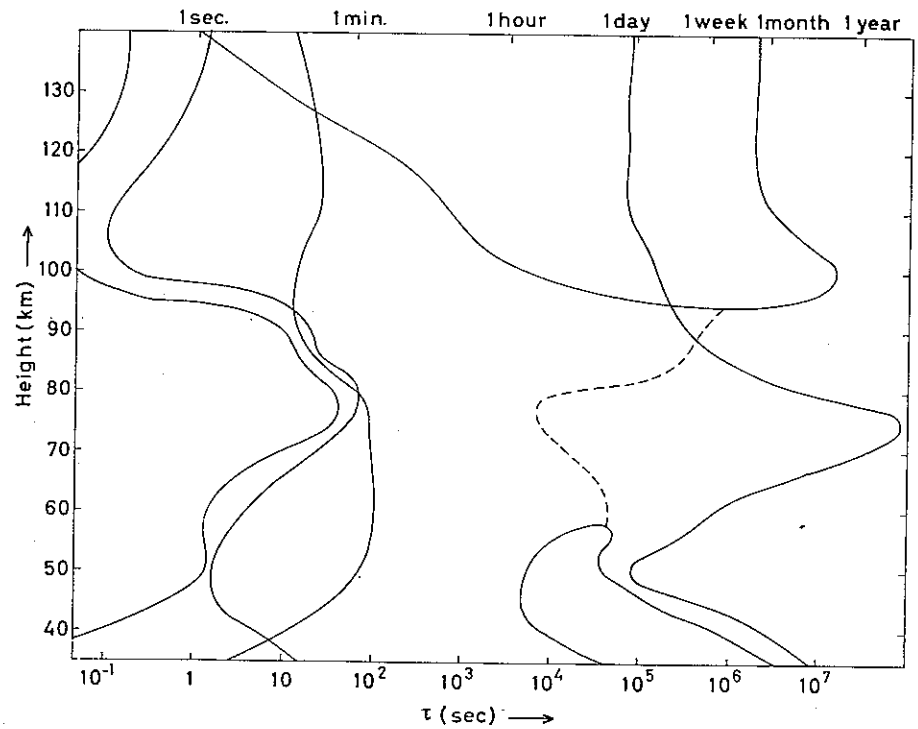

Figure 8. Characteristic times for an oxygen-hydrogen atmosphere (high latitude winter, daytime conditions).

photochemical equilibrium proceeds as damped oscillations. In the case of complex roots the characteristic times, shown in figures 6-8 by dashed lines, were taken as the inverse value of the real part of the root.

It is interesting to compare the trend of the curves for τ_1 and τ_2 in figures 6-8 to the curves shown in figure 2 for the pure oxygen atmosphere. The τ_1 curves in figure 2 are only slightly altered by the introduction of hydrogen, whereas the longest time τ_2 is considerably reduced between 55 and 90 km.

Still we have not determined the coefficients b_{ji} occurring in expressions (5.9) through (5.16). However such computations, which do not involve any serious difficulties, are only of major interest in more detailed studies of special problems and will not be made in this more general survey.

Returning to equations (2.25) through (2.32) let us consider the coefficients A_i, B_i and C_i. These coefficients consist of variable quantities. We shall assume that these quantities are only allowed to vary within certain limits, i.e. the departures from photochemical equilibrium are restricted. This makes it possible to estimate the order of magnitude of the different terms occurring in the coefficients and to select the most important terms. In many cases the system of equations may be reduced considerably. For instance above 100 km and below 55 km the reductions are such that the equations may be integrated analytically with an accuracy which is sufficient for physical and meteorological purposes.

If dashes are used to denote the reduced versions of the coefficients in equations (2.25) through (2.32), the following type of equations is obtained.

$$\frac{dx_i}{dt_i}=A_i'-B_i'x_i \tag{5.17}$$

(For atomic oxygen also a second degree term $C_i'x_i^2$ should be added for levels above 95 km: for OH and H, as well as for O below 95 km, the second degree terms may be neglected throughout as unimportant). As a first approximation, the characteristic time for the component i may be taken as $\tau_i=1/B_i'$ except for the two components occupying the largest amounts of oxygen and hydrogen. For the component occupying the largest amount of oxygen, the characteristic time is taken equal to the characteristic time of the component having the second largest amount. For the component occupying the largest amount of hydrogen a similar procedure is adopted. Physically this means that the oxygen budget is regarded as an interplay, which may often take place through a complex chain of reactions, between the two components having the largest amount of oxygen (and similarly for the hydrogen budget). In this way approximate values for the characteristic times are obtained for all components. These times may differ by orders of magnitude. The values obtained for the "rapid" components may be taken as highly representative. The characteristic times for the "slower" components may be adjusted in the following way: over the time scale corresponding to the characteristic times of the "slower" components, the "rapid" components may be considered as being in continuous equilibrium with the current concentrations of the other compo-

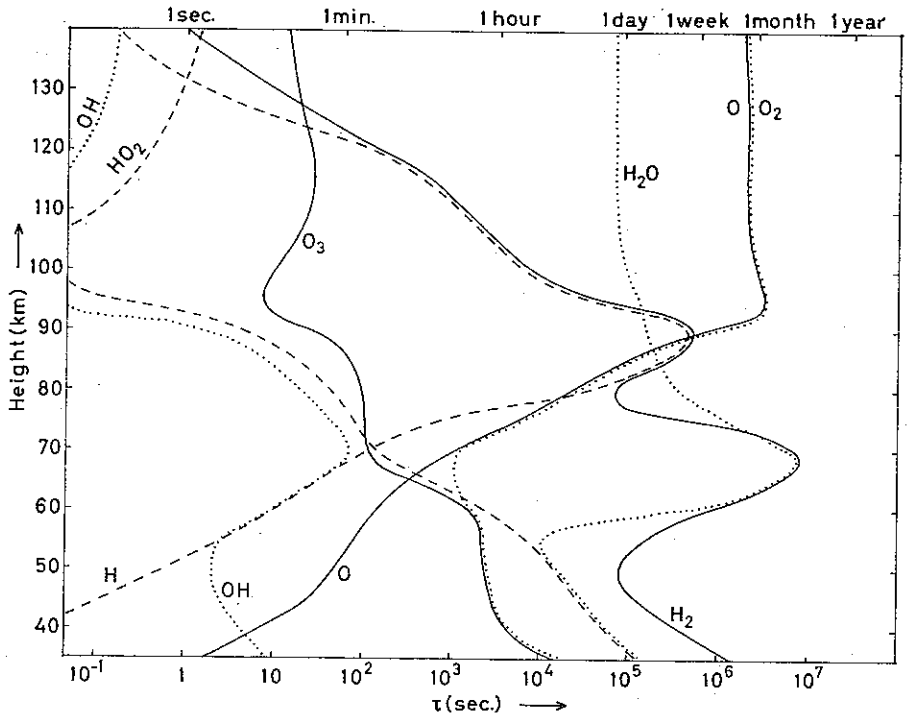

Figure 9. Characteristic times for the eight components of the oxygen-hydrogen atmosphere (low latitude, daytime conditions).

nents. The corresponding differential equations for the rate of change of the concentrations (among the equations 2.25 through 2.32) then reduce to ordinary equations.

Accordingly the concentrations of the "rapid" components may be expressed in terms of the concentrations of the "slower" ones. In some cases the largest terms in A_i' and B_i' cancel each other. This means that the "slower" components have characteristic times still longer than the first approximations evaluated as above.

The mathematical difference between this approach and actually solving the linearized equations is that we have selected the most important term (or terms) in the equations (5.9) through (5.16). In principle the variety of initial perturbations is unlimited, but physically only special combinations of perturbations are likely to occur. This assumption makes it possible to select the most important term in each of the equations (5.9) through (5.16). The results obtained from these two procedures would be only slightly different. Thus a characteristic time may be defined for each component. It should however be emphasized that this is mathematically incorrect. In some cases a selection of the most important term is impossible, since the choice between two (or more) terms may depend upon a choice between two equally probable types of initial perturbations.

Although the introduction of the concept of "characteristic time of a component" may be incorrect in some cases, it is often a very useful mean to visualize the time variations in an atmosphere where the photochemical equilibrium has been disturbed.

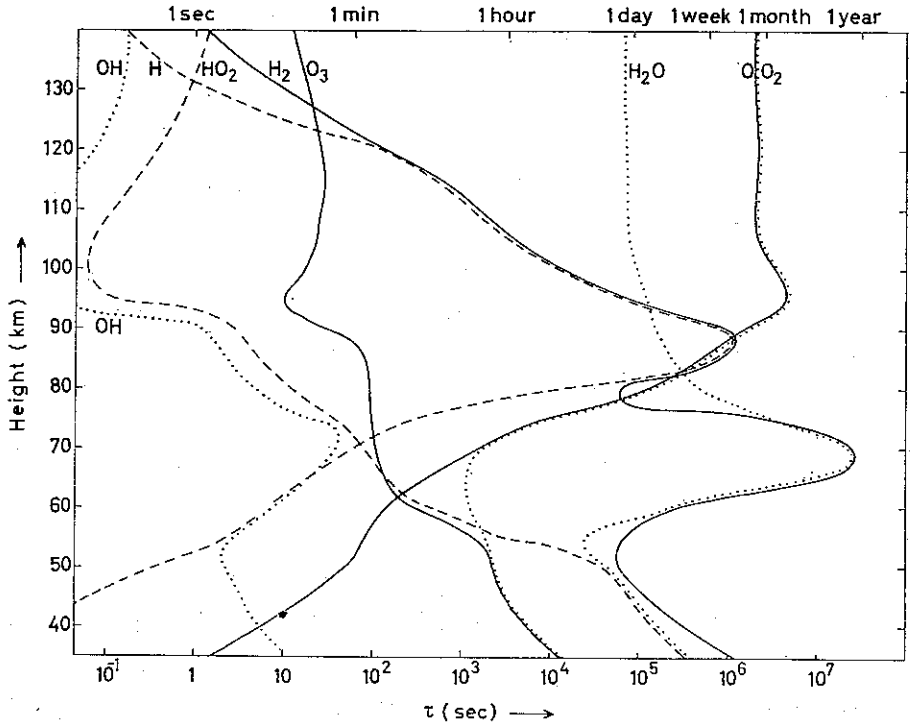

Figure 10. Characteristic times for the eight components of the oxygen-hydrogen atmosphere (high latitude summer, daytime conditions).

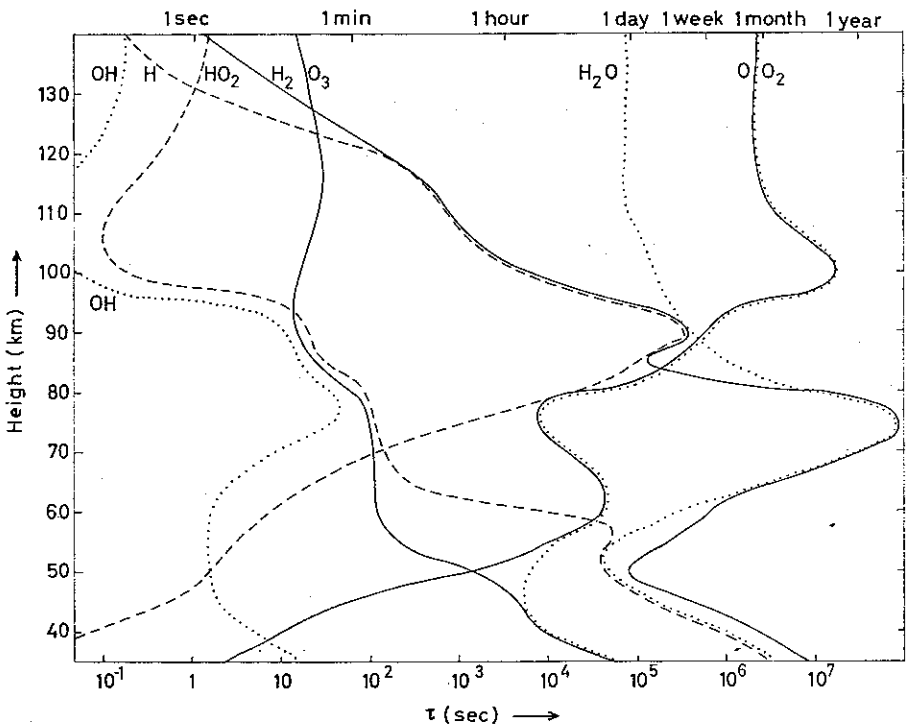

Figure 11. Characteristic times for the eight components of the oxygen-hydrogen atmosphere (high latitude winter, daytime conditions).

The characteristic times, as determined above, are shown in figures 9-11. For reasons mentioned above the curves should only be regarded as "advisory". If we want to study a specific problem the complete equations (5.9) through (5.16) should be used. These may often be reduced, the degree of reduction depending on the typical time scale in our problem.

It has already been mentioned that equations (2.25) through (2.32) may be considerably reduced at certain levels. This reduction is especially pronounced above 105 km and below 55 km.

Below 55 km the pure oxygen components may be treated as if no hydrogen were present. The pure oxygen atmosphere has been discussed earlier (HESSTVEDT, 1963), and the following characteristic times were obtained

(5.18) $$\tau_O \approx 1/k_2[M]\cdot[O_2]$$

(5.19) $$\tau_{O_2} \approx \tau_{O_3} \approx 1/4k_3[O]$$

The equations for the components containing hydrogen may be approximated by

(5.20) $$\frac{d[OH]}{dt} \approx (k_8[O_3]\cdot[H]+k_{11}[O]\cdot[HO_2])-(k_{10}[O]+k_{21}[O_3])\cdot[OH]$$

(5.21) $$\frac{d[HO_2]}{dt} \approx 2(J_{13}[H_2O]+k_{19}[O]\cdot[H_2])-2k_{24}[OH]\cdot[HO_2]$$

(5.22) $$\frac{d[H_2]}{dt} \approx k_{15}[HO_2]\cdot[H]-k_{19}[O]\cdot[H_2]$$

(5.23) $$\frac{d[H_2O]}{dt} \approx (k_{23}[OH]^2+k_{24}[OH]\cdot[HO_2])-J_{13}[H_2O]$$

(5.24) $$\frac{d[H]}{dt} \approx k_{10}[O]\cdot[OH]-(k_7[M]\cdot[O_2]+k_8[O_3])\cdot[H]$$

Accordingly the characteristic times may be approximated by the expressions

(5.25) $$\tau_{OH} \approx 1/(k_{10}[O]+k_{21}[O_3])$$

(5.26) $$\tau_{HO_2} \approx 1/2k_{24}[OH]$$

(5.27) $$\tau_{H_2} \approx 1/k_{19}[O]$$

(5.28) $$\tau_H \approx 1/(k_7[M]\cdot[O_2]+k_8[O_3])$$

Since we will, at these levels, regard the hydrogen budget as an interplay between water vapor and molecular hydrogen, we may write

$$\tau_{H_2O} \approx \tau_{H_2} \approx 1/k_{19}[O] \tag{5.29}$$

Above 105 km the basic equations may be reduced as follows

$$\frac{d[O]}{dt} \approx 2J_2[O_2] - 2k_1[M]\cdot[O]^2 \tag{5.30}$$

$$\frac{d[O_2]}{dt} \approx k_1[M]\cdot[O]^2 - J_2[O_2] \tag{5.31}$$

$$\frac{d[O_3]}{dt} \approx k_2[M]\cdot[O]\cdot[O_2] - (J_3 + k_3[O] + k_8[H])\cdot[O_3] \tag{5.32}$$

$$\frac{d[OH]}{dt} \approx (k_6[M]\cdot[O] + k_{22}[O_2])\cdot[H] - k_{10}[O]\cdot[OH] \tag{5.33}$$

$$\frac{d[HO_2]}{dt} \approx k_7[M]\cdot[O_2]\cdot[H] - k_{11}[O]\cdot[HO_2] \tag{5.34}$$

$$\frac{d[H_2]}{dt} \approx (k_{17}[M]\cdot[H] + k_{18}[OH])\cdot[H] - k_{19}[O]\cdot[H_2] \tag{5.35}$$

$$\frac{d[H_2O]}{dt} \approx k_{14}[HO_2]\cdot[H] - J_{13}[H_2O] \tag{5.36}$$

$$\frac{d[H]}{dt} \approx k_{10}[O]\cdot[H] - (k_6[M]\cdot[O] + k_{22}[O_2])\cdot[H] \tag{5.37}$$

It is seen that the dominant feature of the oxygen budget is the conversion from atomic to molecular oxygen and vice versa. The characteristic times for these components are

$$\tau_O \approx \tau_{O_2} \approx 1/(J_2 + 4k_1[M]\cdot[O]) \tag{5.38}$$

For the remaining components we obtain

$$\tau_{O_3} \approx 1/(J_3 + k_3[O] + k_8[H]) \tag{5.39}$$

$$\tau_{OH} \approx 1/k_{10}[O] \tag{5.40}$$

$$\tau_{HO_2} \approx 1/k_{11}[O] \tag{5.41}$$

(5.42) $$\tau_{H_2} \approx 1/k_{19}[O]$$

(5.43) $$\tau_{H_2O} \approx 1/J_{13}$$

The characteristic time for atomic hydrogen τ_H may be taken equal to τ_{OH} down to about 125 km. Below 125 km H_2 takes over as the most frequent hydrogen compound next to H, and it becomes natural to regard τ_H as equal to τ_{H_2}. Moreover, equation (5.37) should be treated with extreme care since reductions may be made by substitutions from the complete differential equations for components having very short characteristic times. The nature and the effect of these substitutions will depend strongly upon the type of perturbation.

6. Diurnal variations in the oxygen-hydrogen atmosphere. The night-time variations in the oxygen-hydrogen atmosphere model are obtained if we put $\mathcal{J}_2=\mathcal{J}_3=\mathcal{J}_{12}=\mathcal{J}_{13}=0$ in the basic equations. In the preceding sections the day-time conditions have been discussed, assuming the radiation to be constant over a time which is much longer than the longest characteristic time obtained ("infinitely long day"). Similar considerations may be made for an "infinitely long night". However none of these considerations should be regarded as a goal in itself, what we really want to study is the state of the atmosphere during night and day when the radiation is interrupted at intervals of about 12 hours. A 12 hour period is at any level, latitude and season, insufficient for complete day-time or night-time photochemical equilibrium to occur. Consequently the concentrations will oscillate between their day-time and night-time equilibrium values. The character of these oscillations may be entirely different for different levels. If for instance the characteristic times for both night-time and day-time conditions are short (i.e. $\ll$12 hours) then the concentration of a component will rapidly shift from day-time to night-time equilibrium ("equilibrium" is used here to denote that the concentration of the component in question is in photochemical equilibrium with the actual concentrations of the other components). If on the other hand the characteristic time for day-time and/or for night-time are much longer than 12 hours, then the diurnal variations will be negligibly small.

In order to calculate the concentrations and the characteristic times and their variations in the course of a 24 hour period, we shall make some simplifying assumptions about the time variation of solar radiation. During the night the radiation is, of course, taken to be zero; during the day the solar radiation depends on the elevation of the sun from sunrise to sunset. In our calculations we shall assume the elevation to be constant and equal to its mean value in the course of a day. The length of the day is taken to be 12 hours for low latitude, 18 hours for high latitude, summer, and 6 hours for low latitude, winter. The computations were made as follows: the basic equations (2.25) through (2.32) were integrated over the period of darkness (dissociation rates equal to zero) using daytime equilibrium values to determine the coefficients A_i, B_i and C_i, which are regarded as constants during the integration. In this way we obtain two

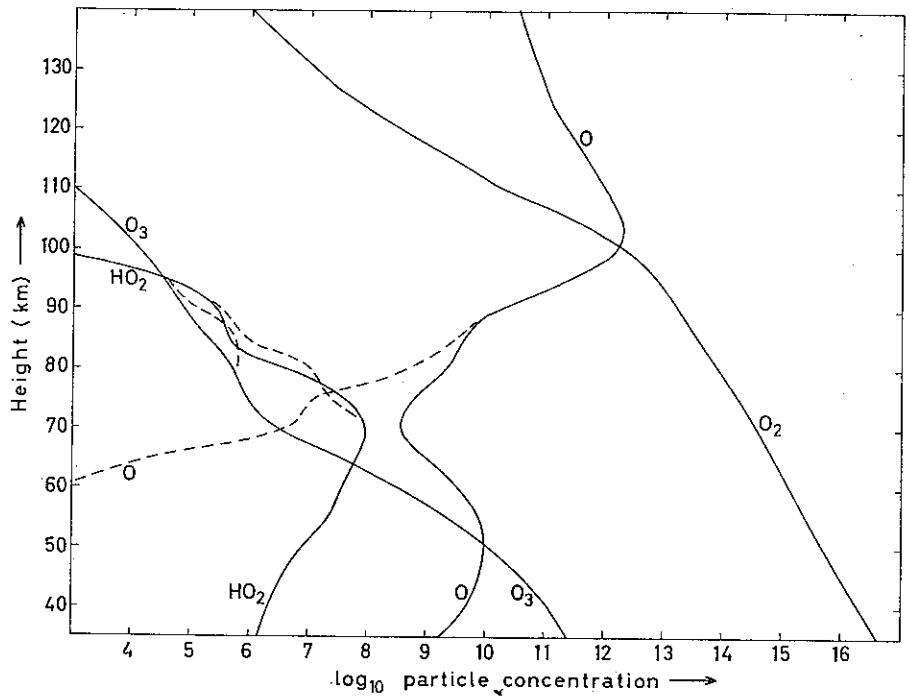

Figure 12. Concentrations of O, O_2, O_3 and HO_2 in an oxygen-hydrogen atmosphere. Where diurnal variations are significant, daytime concentrations are represented by a solid curve and night-time concentrations by a broken curve (low latitude).

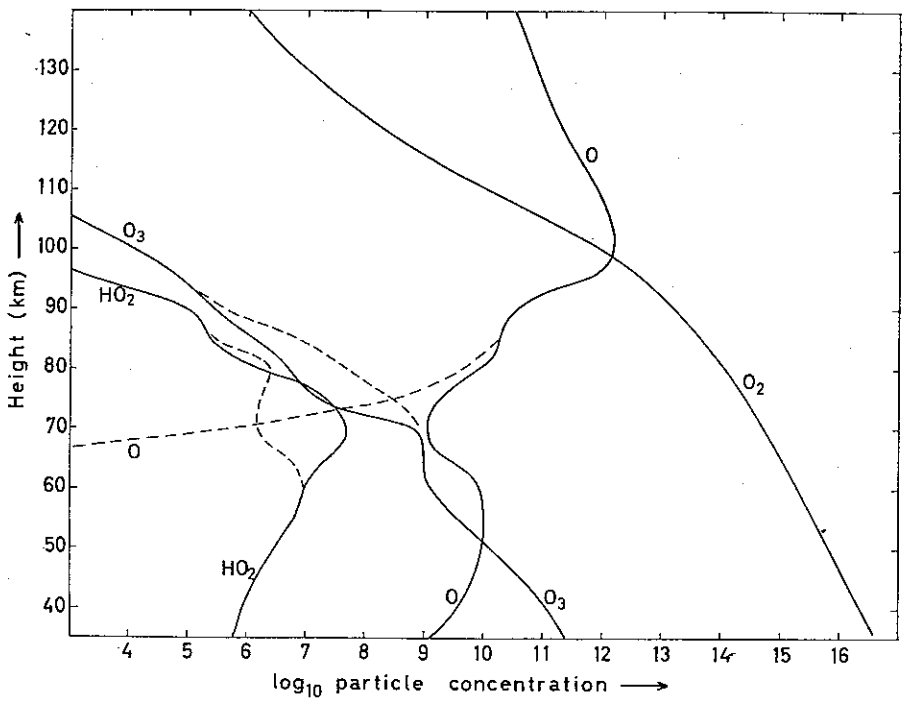

Figure 13. Concentrations of O, O_2, O_3 and HO_2 in an oxygen-hydrogen atmosphere. Where diurnal variations are significant, daytime concentrations are represented by a solid curve and night-time concentrations by a broken curve (high latitude summer).

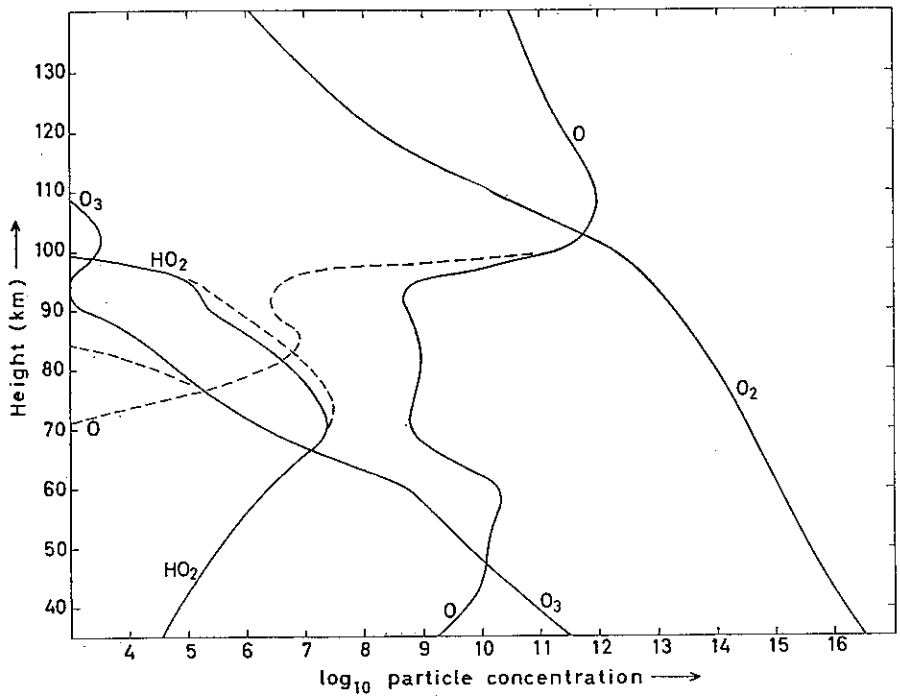

Figure 14. Concentrations of O, O_2, O_3 and HO_2 in an oxygen-hydrogen atmosphere. Where diurnal variations are significant, daytime concentrations are represented by a solid curve and night-time concentrations by a broken curve (high latitude winter).

sets of concentrations, one approximating day-time conditions and one approximating night-time conditions. The integration is then continued over a day, starting with the sunrise concentrations and using day-time values to determine the coefficients A_i, B_i and C_i. This procedure is continued over a series of days and nights until the convergence is satisfactory. This convergence may be considerably speeded up by considering the characteristic times. For instance above 100 km the characteristic times for O and O_2 are very long both for day-time and for night-time conditions. Therefore the diurnal variations are very small and may be neglected. The condition for the variation to be the same for two consecutive 24-hour periods is then:

$$t_d(A_2 - B_2[O_2]) + t_n(A_2^* - B_2^*[O_2]) = 0 \tag{6.1}$$

where A_2 and B_2 are obtained from substitutions of day-time concentrations and A_2^* and B_2^* are obtained from substitutions of night-time concentrations, t_d is the length of the day and t_n is the length of the night. Since B_2^* may be neglected and $A_2 \approx A_2^*$ we obtain

$$[O_2] \approx [O_2]_e \cdot \frac{t_d + t_n}{t_d} \tag{6.2}$$

If the characteristic time for a component is found to be much shorter than the length of the day or night the differential equation for the time variation may be replaced

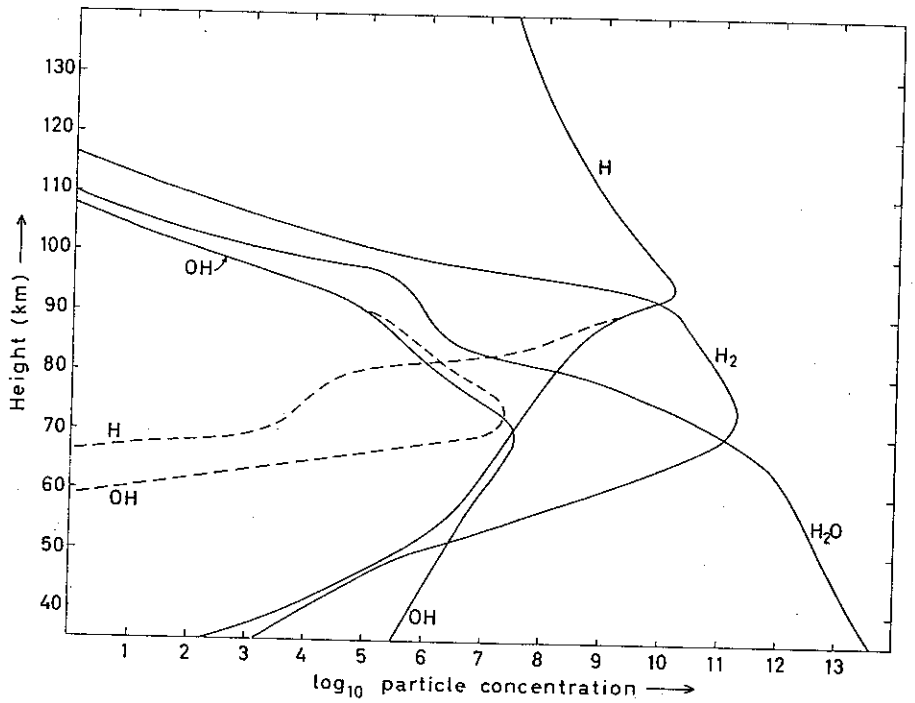

Figure 15. Concentrations of H, H_2, H_2O and OH in an oxygen-hydrogen atmosphere. Where diurnal variations are significant, daytime concentrations are represented by a solid curve and night-time concentrations by a broken curve (low latitude).

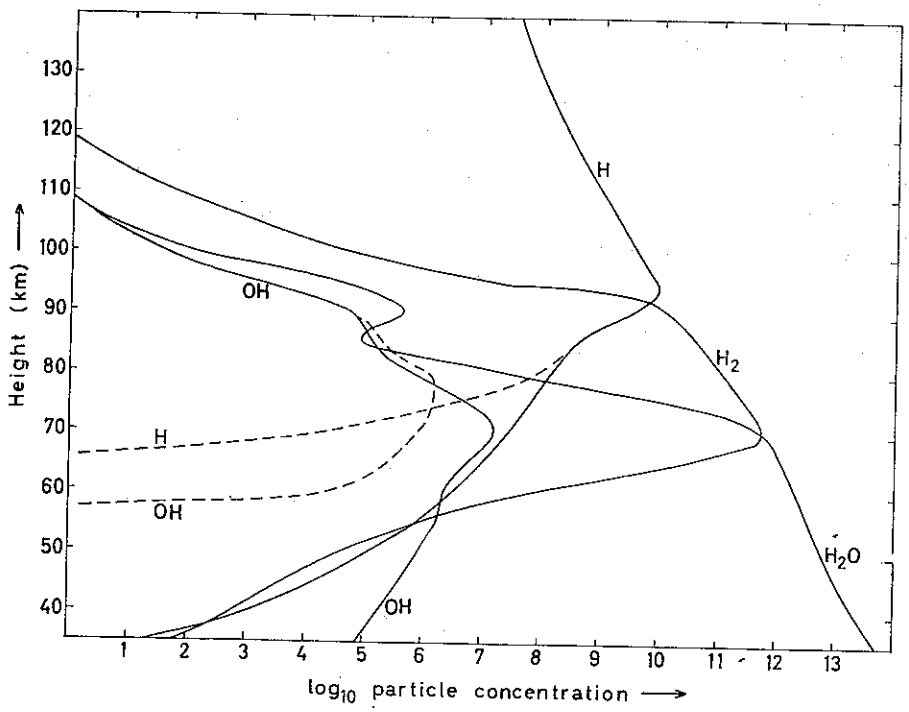

Figure 16. Concentrations of H, H_2, H_2O and OH in an oxygen-hydrogen atmosphere. Where diurnal variations are significant, daytime concentrations are represented by a solid curve and night-time concentrations by a broken curve (high latitude summer).

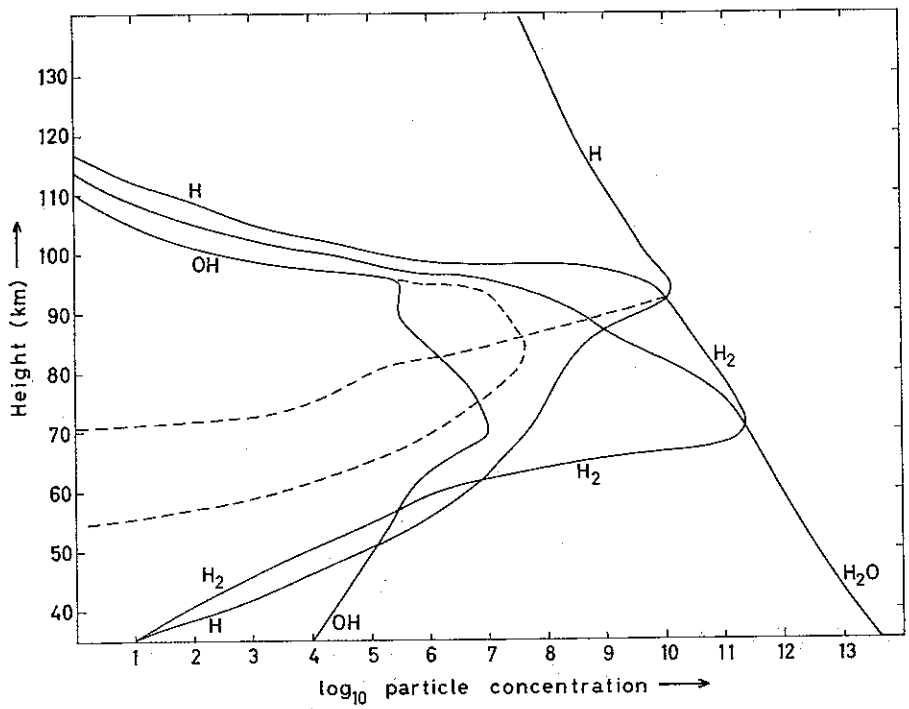

Figure 17. Concentrations of H, H_2, H_2O and OH in an oxygen-hydrogen atmosphere. Where diurnal variations are significant, daytime concentrations are represented by a solid curve and night-time concentrations by a broken curve (high latitude winter).

by an ordinary equation by omitting the differential term. It should also be mentioned again that the concentrations of the components representing the largest amounts of oxygen and hydrogen are always determined from (2.33) and (2.34). Thus, a numerical integration will only be necessary when the characteristic time is comparable to the length of the day or night. Even in this case the concentrations at sunset (x) and sunrise (y) may, with a sufficient degree of accuracy, be determined from

$$x = x_e + (y - x_e)e^{-Bt_d} \tag{6.3}$$

and

$$y = y_e + (x - y_e)e^{-B^* t_n} \tag{6.4}$$

where $x_e = A/B$ and $y_e = A^*/B^*$ are equilibrium values determined from substitution of actual day-time and night-time concentrations. Strictly A, B, A^* and B^* are functions of time, but in most cases this time dependence is not disturbing since the dominating terms very often contain the concentrations only of "very slow" or "very rapid" components.

Using approximations of the indicated type we may avoid slowly converging step-integrations. Day-time concentrations (represented by their values at sunset) and night-time concentrations (represented by their sunrise values) were calculated and the re-

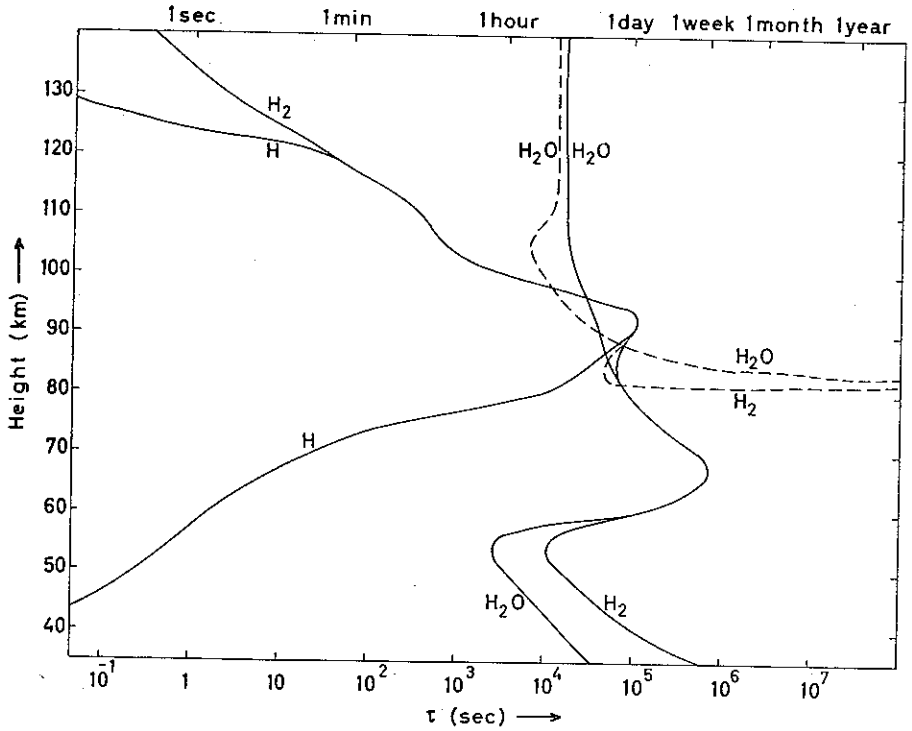

Figure 18. Characteristic times for H, H_2, H_2O in an oxygen-hydrogen atmosphere. If there is a significant difference between the characteristic times during the day and during the night, the former are represented by solid curves, the latter by broken curves (low latitude).

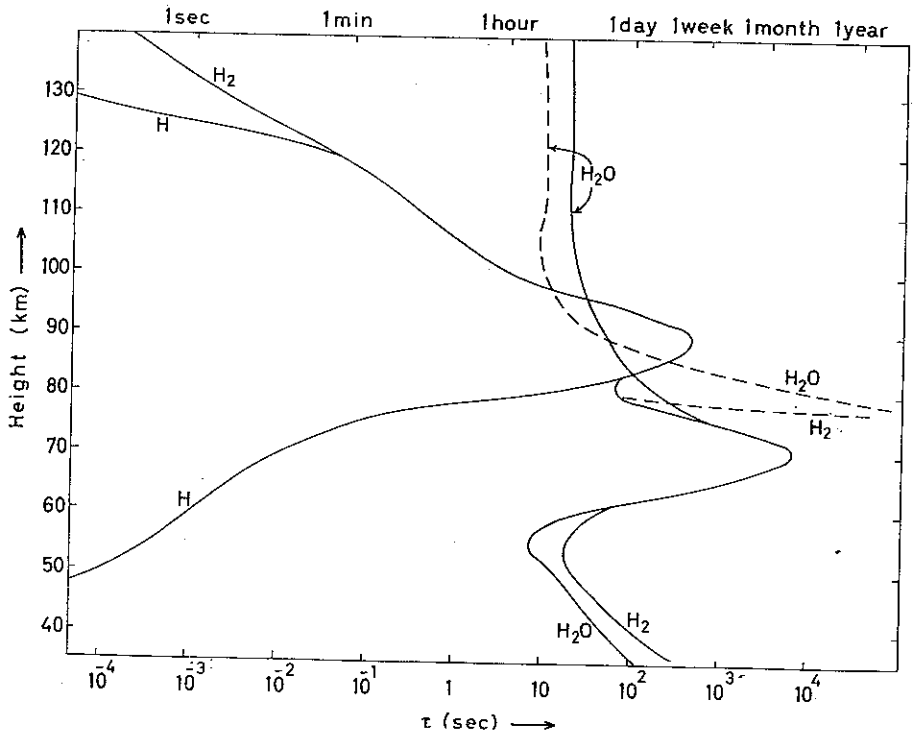

Figure 19. Characteristic times for H, H_2, H_2O in an oxygen-hydrogen atmosphere. If there is a significant difference between the characteristic times during the day and during the night, the former are represented by solid curves, the latter by broken curves (high latitude summer).

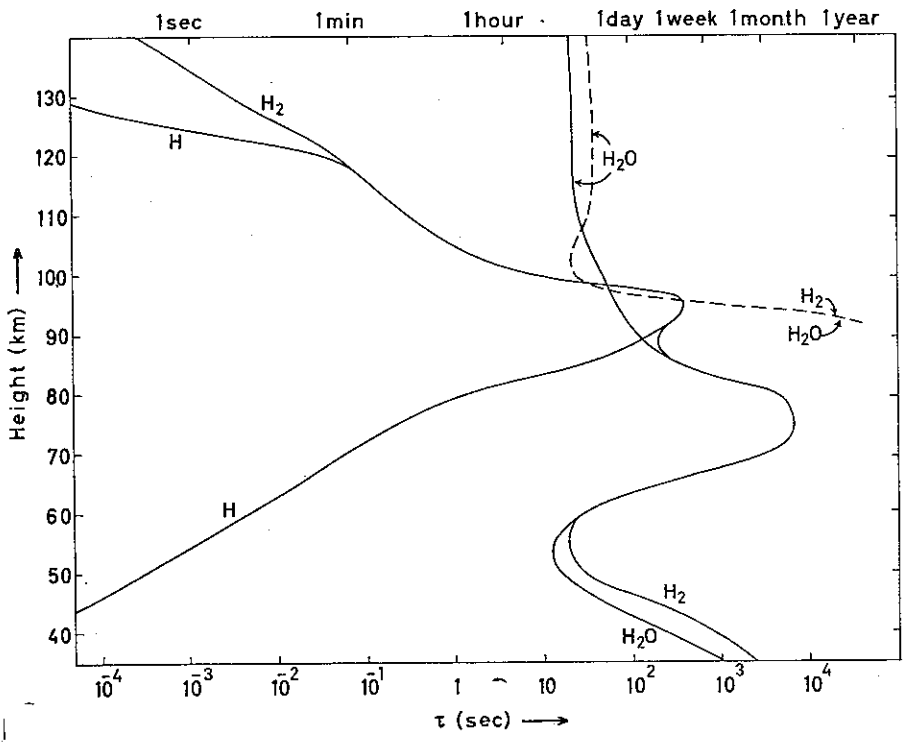

Figure 20. Characteristic times for H, H_2, H_2O in an oxygen-hydrogen atmosphere. If there is a significant difference between the characteristic times during the day and during the night, the former are represented by solid curves, the latter by broken curves (high latitude winter).

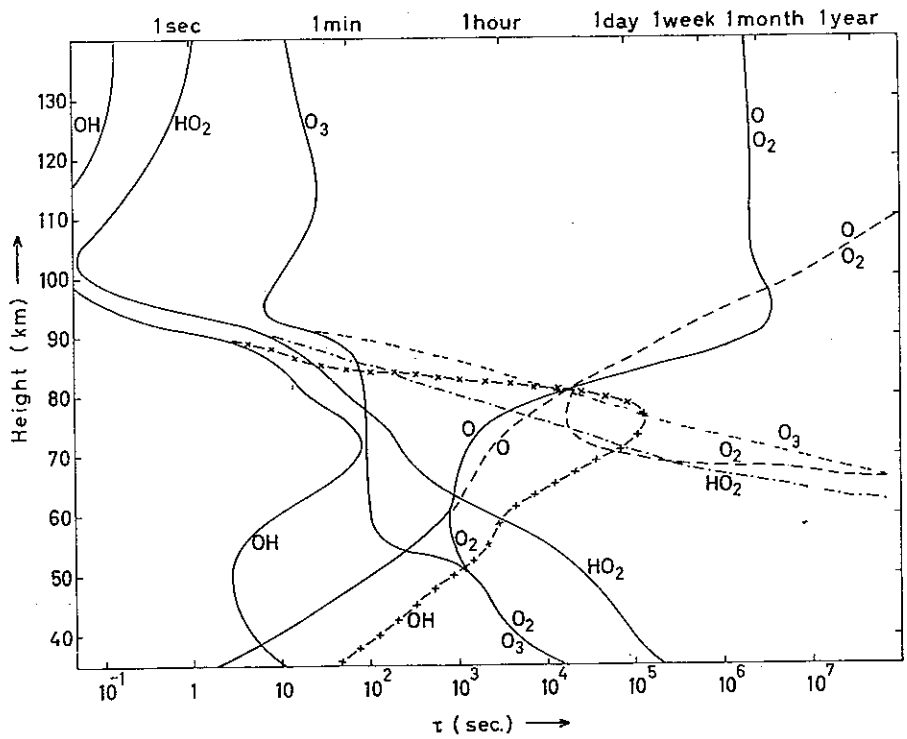

Figure 21. Characteristic times for O, O_2, O_3, OH and HO_2 in an oxygen-hydrogen atmosphere. If there is a significant difference between the characteristic times during the day and during the night, the former are represented by solid curves and the latter by broken curves of different kinds (low latitude).

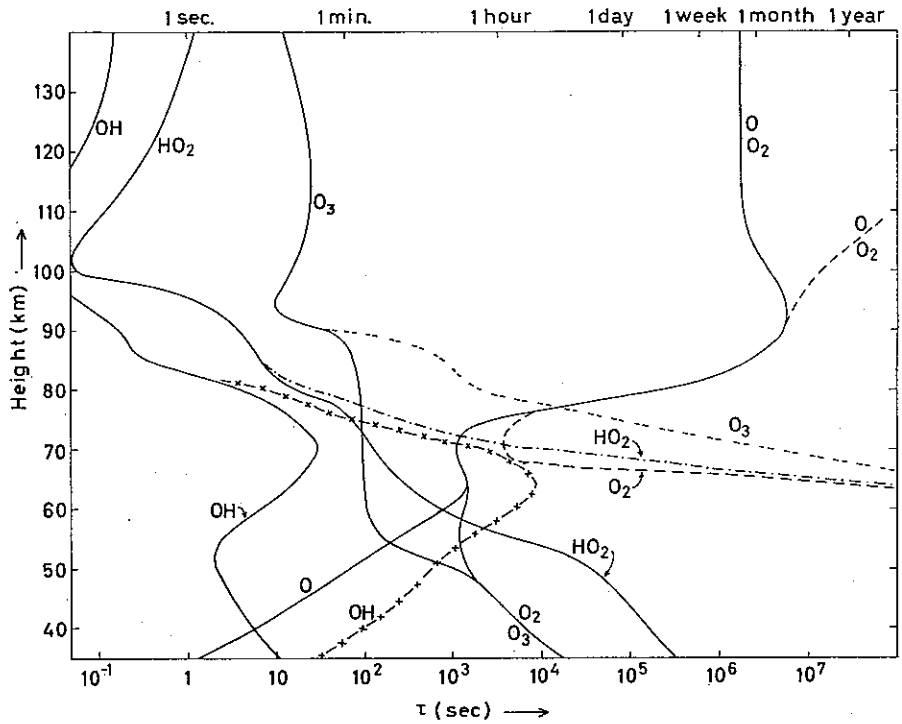

Figure 22. Characteristic times for O, O_2, O_3, OH and HO_2 in an oxygen-hydrogen atmosphere. If there is a significant difference between the characteristic times during the day and during the night, the former are represented by solid curves, the latter by broken curves of different kinds (high latitude summer).

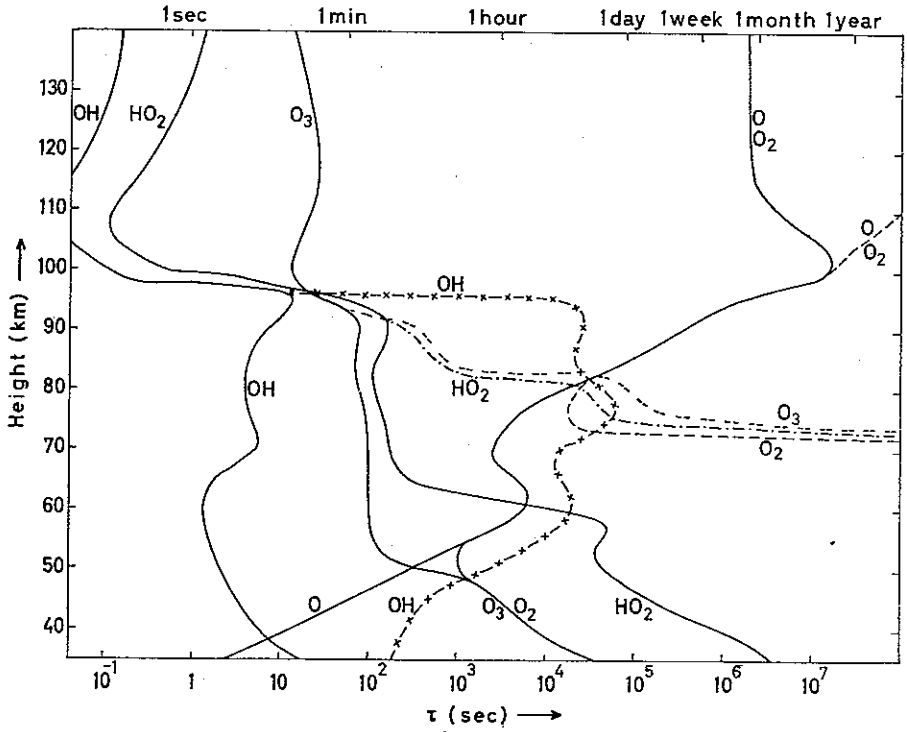

Figure 23. Characteristic times for O, O_2, O_3, OH and HO_2 in an oxygen-hydrogen atmosphere. If there is a significant difference between the characteristic times during the day and during the night, the former are represented by solid curves, the latter by broken curves of different kinds (high latitude winter).

sults are shown in figures 12-17. Furthermore characteristic times for day-time and night-time conditions were determined. The results are shown in figures 18-23. It is seen that the characteristic times during day-time differ only slightly from the values shown in figures 9-11 for day-time equilibrium.

One of the most characteristic features of the oxygen-hydrogen atmosphere is the night-time reduction in the concentrations of O, H and OH below about 70-80 km. As a consequence the lower levels will contribute insignificantly to the total OH*-emission in the nightglow.

It is seen that the diurnal variation of solar radiation does not change the main features of the composition of the atmosphere. The major constituents always have relatively long characteristic times so that the diurnal variations in their concentrations are unimportant. On the other hand the minor constituents very often have short characteristic times and large diurnal variations may be expected.

7. OH* emission in the airglow. Following BATES and NICOLET we shall assume that the OH* emission in the airglow results from recombination of ozone and atomic hydrogen (see equation 2.8). The emission $\triangle E$ per second from a unit volume at a given level is then

$$\Delta E = k_8[O_3]\cdot[H] \tag{7.1}$$

On the basis of the concentrations evaluated in section 6 we may compute $\triangle E$ for our three model atmospheres for day-time (sunset) and night-time (sunrise) conditions. The results are shown in figure 24 (day-time) and 25 (night-time). To start with the OH* emission in the dayglow it is seen that a pronounced maximum occurs between 55 and 60 km. The temperature of these levels is about 260°K. A secondary maximum is found at around 100 km height, the peak value here being more than one order of magnitude lower than the maximum value at 55 km.

The total dayglow emission E from a vertical column of air of cross-section 1 cm^2 is easily obtained by integration. The following values were found:

low latitude	6×10^{10} photons/cm^{2}sec
high latitude summer	7×10^{10} photons/cm^{2}sec
high latitude winter	3×10^{10} photons/cm^{2}sec

It follows that the emission is of the same order of magnitude for the three model atmospheres. A decrease by a factor of 2 was found for high latitudes during the winter. The results indicate no meridional variation during the summer; during the winter a decrease in the emission should be expected for high latitudes. In low latitudes no seasonal variation is likely to occur; in high latitudes the emission should have a maximum during the summer and a minimum during the winter.

From figures 18-20 we see that at the levels of maximum OH* dayglow emission the characteristic time for atomic hydrogen is only a small fraction of a second. From figures 21-23 it follows that the characteristic time for ozone is of the order of magnitude

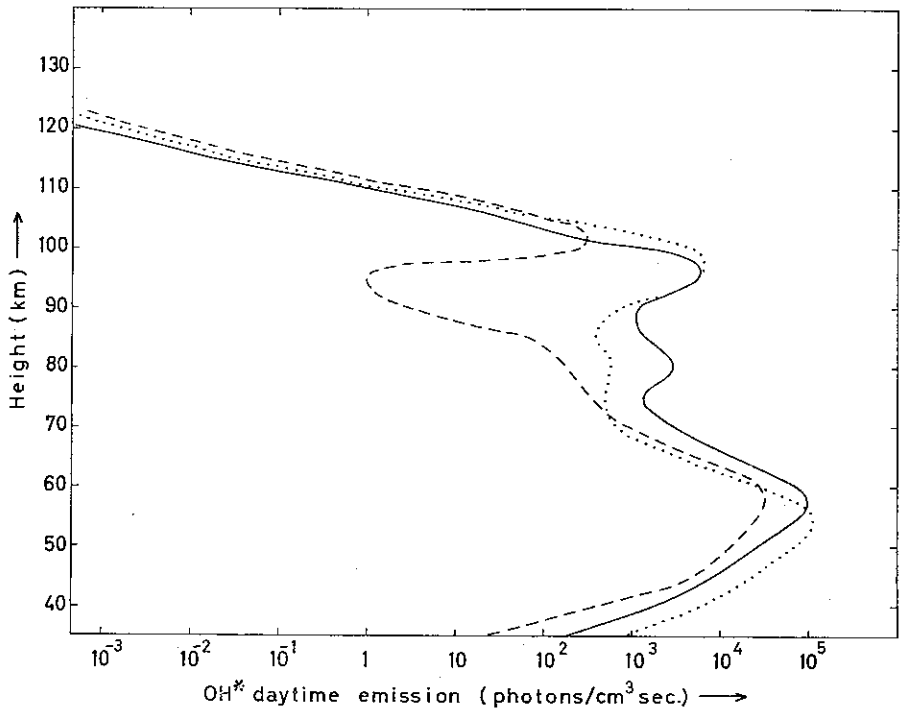

Figure 24. Calculated OH* dayglow emission, based on the assumption of a static atmosphere model (solid curve: high latitude summer, broken curve: high latitude winter, dotted curve: low latitude).

of a few minutes during the day and very long during the night. H and O_3 may then be regarded as being in photochemical equilibrium with the actual concentrations of the other components. Consequently the OH* emission will immediately increase from zero at sunrise to a daytime value which probably varies little with the elevation of the sun.

Due to the rapid recombination of atomic oxygen and atomic hydrogen below about 70 km the OH* emission from this lower part of the atmosphere is negligibly small. As is shown in figure 25, maximum nightglow emission comes from the levels where we found the secondary maximum in the dayglow emission, i.e. around 95 km. In general the emission is stronger during the night than during the day because of the nocturnal increase in the ozone amount.

The height of maximum emission, as well as the total nightglow emission from a vertical column of air, is seen to depend rather strongly upon the features of the model atmosphere. For low latitudes the level of maximum emission was found at 97 km where the temperature is about 210°K. In high latitudes the level of maximum emission sinks to 82 km (with a temperature of 160°K) during the summer, whereas the emission during the winter has its maximum as high as 102 km (with a temperature of 250°K). For the total nightglow emission the following data were obtained

low latitude	5×10^3 photons/cm^{2}sec
high latitude summer	2×10^{10} photons/cm^{2}sec
high latitude winter	2×10^9 photons/cm^{2}sec

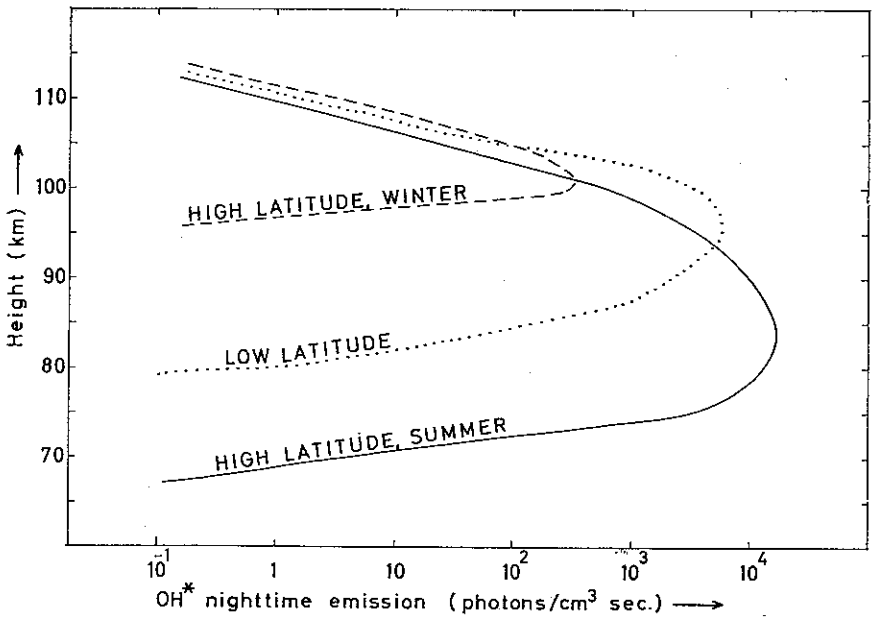

Figure 25. Calculated OH* nightglow emission, based on the assumption of a static atmosphere model (solid cruve: high latitude summer, broken curve: high latitude winter, dotted curve: low latitude).

It is remarkable that, in our model atmospheres for high latitudes the OH*-emission is two orders of magnitude weaker during the winter than during the summer. It should however be emphasized that theoretical computations depend rather strongly upon the data chosen for the model atmosphere: temperature and pressure profile, length of the day, elevation of the sun and the fractional content of hydrogen. Furthermore the results obtained so far refer to static model atmospheres. As will be shown in section 8, the circulation of the atmosphere will influence the nightglow emission rather strongly. On the other hand the dayglow data obtained for the maximum levels around 55 km will be only slightly altered by the consideration of the movement of the air.

8. Influence of the circulation of the air upon the OH* airglow emission. A model for the general circulation in the high atmosphere has been computed by MURGATROYD and SINGLETON (1961). In order to obtain an impression of to what extent the results derived above for static model atmospheres are altered by considering the movement of the air we shall adopt the circulation models proposed by these authors (see also HESSTVEDT, 1964).

Let us start with the dayglow emission from the levels where we found the main maximum, i.e. around 55 km. According to MURGATROYD and SINGLETON the meridional air transport is here directed from the summer hemisphere to the winter hemisphere. The velocity increases rapidly with height from a very small value at 50 km to around 5-10 km/hour at 60 km. Since the characteristic times for O_3 and H are of the order of minutes or even shorter, the effect of a meridional transport should be unimportant. Furthermore the circulation model prescribes an upward motion in the

summer hemisphere and downward motion in the winter hemisphere. The highest values (in high latitudes) of the vertical transport below 60 km is of the order of 40 m/hour. Thus the movement of the air will have no influence upon the OH* dayglow emission at levels around the maximum at the 55 km level.

On the other hand the circulation of the atmosphere may turn out to influence the intensity of the OH* airglow emission at the levels 80-100 km, where we have the maximum emission in the nightglow. On the basis of equations (2.25) through (2.32) and a circulation model it is possible to evaluate numerically the modification caused by the movement of the air. This will not be done in the present paper. Here we shall confine ourselves to a crude estimation of the magnitude of the effect to demonstrate the necessity of involving the circulation in future photochemical atmospheric models.

Let us assume a circulation which prescribes ascending motion in the polar region during the summer, horizontal advection in lower latitudes across the equator to the winter hemisphere, and descending motion in the polar region during the winter. Approximate values for the vertical and horizontal velocities may be obtained from extrapolation of MURGATROYD and SINGLETON's data. Furthermore we shall assume that the characteristic times for atomic oxygen are equal to those given in figures 12-14. (This is a very crude approximation, since the problem is non-linear). By multiplication we obtain approximate values for the distances travelled during the characteristic time for atomic oxygen, which is the most sensitive factor in the expression for the OH* nightglow emission. The results should then be compared to the vertical profiles of the mixing ratios [O]/[M] to give an estimate of the effect of the airmotion.

It turns out that for high latitude summer the results obtained for the static model are somewhat modified between 80 and 100 km. However the degree of reduction is very hard to estimate on the basis of the data at hand. We see from figure 13 that the characteristic time for atomic oxygen varies strongly with height, i.e. with the concentrations of the other components, so that even small variations in these concentrations may change the characteristic time considerably. Furthermore the velocity data are poorly known at these levels. Thus our only conclusion is that the circulation makes it necessary to modify the results obtained for the static model.

A similar reasoning for the meridional transport from high latitudes in the summer hemisphere to high latitudes in the winter hemisphere shows that also for low latitude and high latitude winter the results obtained for the static model are influenced by the motion of the air. The magnitude of this modification is difficult to give because of the assumptions made above, but it is believed that the results obtained for the static model are not misleading for low latitudes. As for the high latitude winter atmosphere the modification is likely to be large at the levels of maximum OH* emission. The total intensity is likely to be considerably increased and the level of maximum emission lowered by about 5 km.

Finally the effect of the descending motion in the polar winter atmosphere is likely to lower the level of maximum emission by another 5 km and also to increase further the total intensity.

These considerations clearly show that no future study of the OH* (and Na) nightglow emission should be made without considering the effect of atmospheric circulation. Numerical computations for such model atmospheres are highly desireable.

REFERENCES

BALLIF, J. R., and S. V. VENKATESWARAN, 1963: On the temporal variations of the OH nightglow. *J. Atmos. Sci.*, **20**, 1-4.

BATES, D. R., and M. NICOLET, 1950: The photochemistry of atmospheric water vapor. *J. Geophys. Res.*, **55**, 301-327.

DÜTSCH, H. U., 1956: Atmosphärisches Ozon als Indikator für Strömungen in der Stratosphäre. *Arch. Meteor., Geophys. und Biokl.*, A, 9, 87-119.

FRIEDMAN, H., 1961: Lyman-α Radiation, *IAGA Symposium No. 1, Symposium d' Aéronomie, Communications présentées à la réunion de Copenhague, Juillet 1960.* 30-33.

GUTNICK, M., 1962: Mean annual mid-latitude moisture profiles to 31 km. *Air Force Surveys in Geophysics*, No. 147.

HESSTVEDT, E., 1963: On the determination of characteristic times in a pure oxygen atmosphere. *Tellus*, **15**, 82-88.

HESSTVEDT, E., 1964: On the water vapor content in the high atmosphere. Geofys. Publ., **25**, No. 3, 1-18.

MURGATROYD, R. J., and F. SINGLETON, 1961: Possible meridional circulations in the stratosphere and mesosphere. *Quart. J. R. Meteor. Soc.*, **87**, 125-135.

NAWROCKI, P. J. and R. PAPA, 1961: *Atmospheric processes*, Geophysics Corporation of America, GCA 61-37-A, Bedford, Mass.

NICOLET, M., 1958: Aeronomic conditions in the mesosphere and lower thermosphere. *Ionospheric Research, Scientific Report* No. 102, Pennsylvania State University.

NORDBERG, W., and W. G. STROUD, 1961: Results of IGY rocketgrenade experiments to measure temperature and winds above the Island of Guam. *J. Geophys. Res.*, **66**, 455-464.

WALLACE, L., 1962: The OH nightglow emission. *J. Atmos. Sci.*, **19**, 1-16.

WATANABE, K., 1958: Ultraviolet absorption processes in the upper atmosphere. *Advances in geophysics*, **5**, 153-221.

Avhandlinger som ønskes opptatt i «Geofysiske Publikasjoner», må fremlegges i Videnskaps-Akademiet av et sakkyndig medlem.

Vol. XXI.

No. 1. A. Omholt: Studies on the excitation of aurora borealis II. The forbidden oxygen lines. 1959.
» 2. Tor Hagfors: Investigation of the scattering of radio waves at metric wavelengths in the lower ionosphere. 1959.
» 3. Håkon Mosby: Deep water in the Norwegian Sea. 1959.
» 4. Søren H. H. Larsen: On the scattering of ultraviolet solar radiation in the atmosphere with the ozone absorption considered. 1959.
» 5. Søren H. H. Larsen: Measurements of amospheric ozone at Spitsbergen (78°N) and Tromsø (70°N) during the winter season. 1959.
» 6. Enok Palm and Arne Foldvik: Contribution to the theory of two-dimensional montain waves 1960.
» 7. Kaare Pedersen and Marius Todsen: Some measurements of the micro-structure of fog and stratus-clouds in the Oslo area. 1960.
» 8. Kaare Pedersen: An experiment in numerical prediction of the 500 mb wind field. 1960.
» 9. Eigil Hesstvedt: On the physics of mother of pearl clouds. 1960.

Vol. XXII.

No. 1. L. Harang and K. Malmjord: Drift measurements of the E-layer at Kjeller and Tromsø during the international geophysical year 1957—58. 1960.
» 2. Leiv Harang and Anders Omholt: Luminosity curves of high aurorae. 1960.
» 3. Arnt Eliassen and Enok Palm: On the transfer of energy in stationary mountain waves. 1961.
» 4. Yngvar Gotaas: Mother of pearl clouds over Southern Norway, February 21, 1959. 1961.
» 5. H. Økland: An experiment in numeral integration of the barotropic equation by a quasi-Lagrangian method. 1962.
» 6. L. Vegard: Auroral investigations during the winter seasons 1957/58—1959/60 and their bearing on solar terrestrial relationships. 1961.
» 7. Gunnvald Bøyum: A study of evaporation and heat exchange between the sea surface and the atmosphere. 1962.

Vol. XXIII.

No. 1. Bernt Mæhlum: The sporadic E auroral zone. 1962.
» 2. Bernt Mæhlum: Small scale structure and drift in the sporadic E layer as observed in the auroral zone. 1962.
» 3. L. Harang and K. Malmjord: Determination of drift movements of the ionosphere at high latitudes from radio star scintillations. 1962.
» 4. Eyvind Riis: The stability of Couette-flow in non-stratified and stratified viscous fluids. 1962.
» 5. E. Frogner: Temperature changes on a large scale in the arctic winter stratosphere and their probable effects on the tropospheric circulation. 1962.
» 6. Odd H. Sælen: Studies in the Norwegian Atlantic Current. Part II: Investigations during the years 1954—59 in an area west of Stad. 1963.

Vol. XXIV.

In memory of Vilhelm Bjerknes on the 100th anniversary of his birth. 1962.

Vol. XXV.

No. 1. Kaare Pedersen: On the quantitative precipitation forecasting with a quasi-geostrophic model. 1963.
» 2. Peter Thrane: Perturbations in a baroclinic model atmosphere. 1963.
» 3. Eigil Hesstvedt: On the water vapor content in the high atmosphere. 1964.
» 4. Torbjørn Ellingsen: On periodic motions of an ideal fluid with an elastic boundary. 1964.
» 5. Jonas Ekman Fjeldstad: Internal waves of tidal origin. 1964.
» 6. A. Eftestøl and A. Omholt: Studies on the excitation of N_2 and N_2^+ bands in aurora. 1965.

A.s John Griegs Boktrykkeri